Journal of Power Sources 251 (2014) 264–268

Contents lists available at ScienceDirect

Journal of Power Sources

journal homepage: www.elsevier.com/locate/jpowsour

Short communication

Facile synthesis and electrochemical properties of two dimensional layered MoS_2/graphene composite for reversible lithium storage

Xinfa Zhou [a,b], Zhen Wang [a], Weixiang Chen [a,*], Lin Ma [a], Dongyun Chen [c], Jim Yang Lee [c]

[a] Department of Chemistry, Zhejiang University, Hangzhou 310027, China
[b] Zhejiang Institute of Energy and Nuclear Technology Application, Hangzhou 310021, China
[c] Department of Chemical and Biomolecular Engineering, National University of Singapore, Singapore 119260, Singapore

HIGHLIGHTS

- A facile method suitable for the large-scale production of 2D layered MoS_2/graphene composite.
- Good dispersion of 2D MoS_2 with ~6 layers on the surface of crumpled graphene nanosheets.
- Excellent electrochemical properties of the MoS_2/graphene composite as a reversible lithium storage host.

GRAPHICAL ABSTRACT

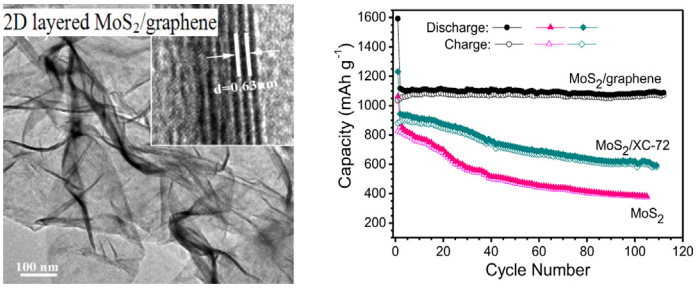

ARTICLE INFO

Article history:
Received 1 October 2013
Received in revised form
5 November 2013
Accepted 15 November 2013
Available online 1 December 2013

Keywords:
Molybdenum disulfide nanosheets
Graphene
Composites
Lithium storage

ABSTRACT

Two dimensional (2D) layered MoS_2/graphene and MoS_2/XC-72 composites are synthesized by a facile aqueous reduction and heat treatment in N_2, and characterized by XRD, SEM, TEM and HRTEM. It is found that the 2D MoS_2 nanosheets with ~6 layers are well dispersed on the crumpled graphene surface and the curved layered MoS_2 with ~10 layers coated on XC-72 carbon. Due to the outstanding properties of graphene and the synergistic interaction between 2D MoS_2 and graphene nanosheets, the 2D MoS_2/graphene composite exhibits a very high reversible capacity of 1060 mAh g^{-1} with excellent cycle stability and significantly enhanced rate capability compared with pristine MoS_2 and the MoS_2/XC-72 composite. The synthesis presented in this work can also be the blueprint for the facile production of the 2D MoS_2/graphene composite on a relatively large scale.

© 2013 Elsevier B.V. All rights reserved.

1. Introduction

Li-ion batteries (LIBs) are found in innumerable portable electronic devices, but their energy and power densities, cycle life and rate capability have to be improved to meet the more demanding specifications of power-intensive applications such as the electric vehicles. The performance of LIBs is largely dependent on the electrode materials and new materials such as graphene nanosheets, with their excellent electrical conductivity, high charge mobility, large specific surface area and intrinsic material flexibility [1–3], are clearly of interest to battery applications. Composites of graphene with metal or metal oxide nanomaterials (such as Sn, SnO_2 and Co_3O_4) are good prospects to succeed graphite as next generation LIB anodes due to a combination of high specific capacity, and good display of cycle stability and rate capability [4–8].

2D MoS_2 nanosheets have also demonstrated a very large intrinsic capacity (much higher than that of graphite anodes) for the electrochemical storage of lithium [9–11]. Due to their graphene-like structure, 2D MoS_2 nanosheets are structurally more compatible with graphene than 0D nanoparticles and 1D nanorods

* Corresponding author. Tel.: +86 571 87952477; fax: +86 571 87951895.
E-mail address: weixiangchen@zju.edu.cn (W. Chen).

0378-7753/$ – see front matter © 2013 Elsevier B.V. All rights reserved.
http://dx.doi.org/10.1016/j.jpowsour.2013.11.060

are with graphene. Thus, Graphene (or graphene oxide) sheets can be used as an attractive platform for the selective growth of 2D layered MoS_2. The integration of two different but similarly structured nanosheets should result in stable composites with greater versatility and more persistent performance enhancements. MoS_2/graphene composites have demonstrated enhanced electrochemical properties for lithium storage [12,13] and high electrocatalytic activity for the hydrogen evolution reaction [14]; and the enhancement has been attributed to the synergistic interaction between MoS_2 and graphene [12–16]. Indeed heterostructures constructed from different 2D nanosheets are attracting attention because of the display of some unusual properties with a strong application potential [17,18]. Hence significant efforts have been devoted to the synthesis of graphene-2D nanosheet (such as MoS_2 and WS_2) heterostructures. We have previously synthesized few-layer MoS_2/graphene composites by the L-cysteine-assisted hydrothermal method [12]. Li et al. also reported the solvothermal synthesis of MoS_2/RGO (reduced graphene oxide) hybrids [14]. The main disadvantage of hydrothermal and solvothermal processing is the use of high temperature (200–240 °C) and high pressure, which can be aggressive to the processing equipment and adds to the energy cost. Chemical exfoliation is another general approach. For example, Xiao et al. prepared MoS_2 nanosheets/poly(ethylene oxide) composites by the hydrolysis–exfoliation of lithiated MoS_2 in an aqueous PEO solution [9]. Graphene was later added to the PEO solution to improve the rate performance of the composites [14]. Exfoliation processes often require the molybdenum disulfide to be lithiated in advance; typically by n-butyllithium in hexane. A large quantity of organic solvent (hexane) and air-sensitive chemical (*n*-butyllithium) are consumed resulting in an increased process environmental footprint. Recently Zhou et al. reported the synthesis of MoS_2 nanosheet-graphene hybrids by combining an electrochemical lithiation-assisted exfoliation process with a hydrazine monohydrate vapour reduction technique [15]. This electrochemical lithiation-assisted exfoliation process is also sensitive to air and water. The development of large-scale and low-cost production of 2D layered MoS_2/graphene composites is still a challenge up to now.

We present here an alternative method to synthesize 2D layered MoS_2/graphene composites by the simultaneous reduction of $(NH_4)_2MoS_4$ and GOS with hydrazine hydrate in the aqueous phase. The reduction reaction is facile and can be carried out below 100 °C, thereby circumventing the hostile high-temperature and high-pressure environment of hydrothermal (or solvothermal) synthesis; and the excessive use of solvent and the air and water sensitivity of typical lithiation–exfoliation processing of molybdenum disulfide [12–15]. Electrochemical measurements indicated that 2D MoS_2/graphene composite synthesized as such has higher reversible capacity (~1060 mAh g^{-1}), good cycle stability and significantly enhanced high-rate capability compared with pristine MoS_2 and a typical MoS_2/carbon composite.

2. Experimental

2.1. Synthesis and characterization of MoS_2/graphene composite

Graphene oxide sheets (GOS, 5.37 mmol) prepared from graphite powder by a modified Hummers' method [12,19] were dispersed into 100 mL deionized water. 50 mL aqueous solution of $(NH_4)_2MoS_4$ (2.68 mmol) and 10 mL of hydrazine hydrate (85%) were introduced to the GOS suspension. Afterwards, the mixture was transferred to a 250-mL round bottom flask and refluxed at 95 °C for 8 h, during which MoS_4^{2+} and GOS were simultaneously reduced to MoS_2 and graphene, respectively. The solid product was recovered by centrifugation and washed with deionized water, then dried at 80 °C in vacuum. The 2D layered MoS_2/garphene composite was finally obtained by annealing of as-prepared solid product at 800 °C for 2 h in nitrogen. In the controlled experiment, MoS_2/XC-72 composite was prepared using Vulcan XC-72 carbon nanoparticles (CAS RN. 1333-86-4, Cabot Corporation) by the similar route. The mole ratio of $(NH_4)_2MoS_4$ to graphene or XC-72 in the

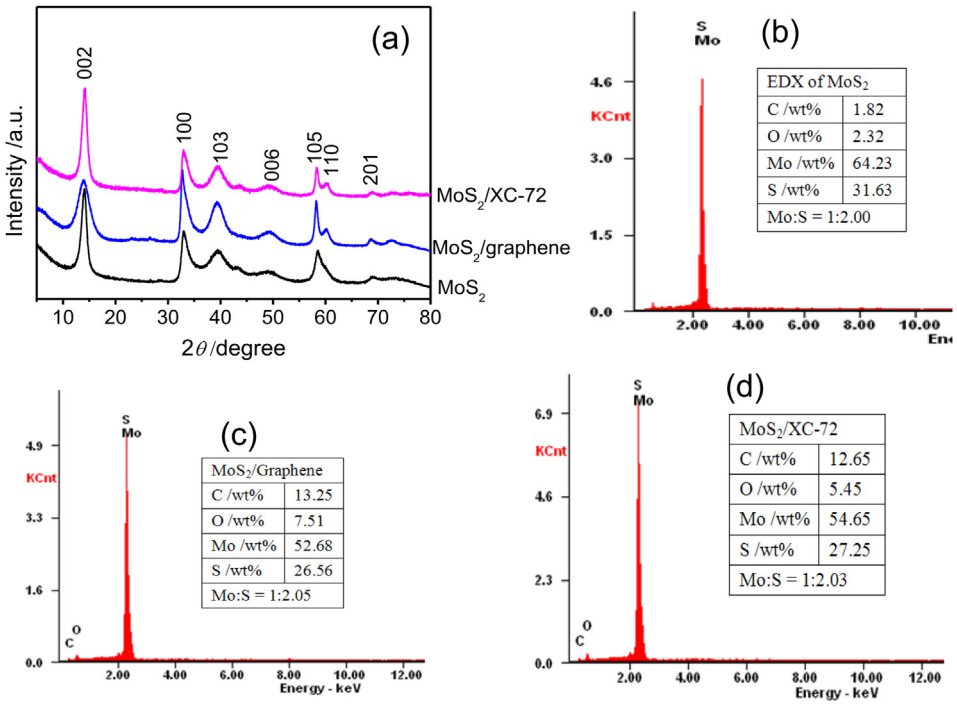

Fig. 1. (a) XRD patterns and (b–d) EDX of the pristine MoS_2, 2D layered MoS_2/graphene and MoS_2/XC-72 composites prepared by facile aqueous reduction after heat treatment. The inserted table lists the element composition of the samples (Mo: S represents the atomic ratio).

starting materials was about 1:2. MoS_2 was also prepared without GOS or Vulcan XC-72 carbon.

XRD was recorded on a Bruker D8 ADVANCE X-ray diffractometer with Cu Kα radiation ($\lambda = 0.15405$ nm). SEM images were taken on a SIRION-100 field emission scanning electron microscope. TEM and HRTEM were carried out on a JEOL JEM-200CX microscope operated at 200 kV. The elemental composition of the samples was examined by energy dispersive X-ray spectroscopy (EDX, GENENIS-4000).

2.2. Electrochemical measurements

The working electrode was fabricated by following process: the slurry consisting of 80 wt% active material, 10 wt% acetylene black and 10 wt% polyvinylidene fluoride was coated on a copper foil (15 mm in diameter, active material loading of about 1.2 mg), then the coated electrode was dried at 120 °C in vacuum for 12 h and compressed. The two-electrode test cells were assembled in an argon-filled glove box using a lithium sheet as the counter electrode, a polypropylene film (Celgard-2300) separator, and an electrolyte of 1.0 M $LiPF_6$ solution in a 1:1 v/v mixture of ethylene carbonate/dimethyl carbonate. Galvanostatic charging/discharging cycle between 0.005 and 3.0 V was carried out on LANHE 2001CA Battery Tester. Electrochemical impendence spectroscopy (EIS) was carried out on a PARSTAR 2273 by applying a sine wave with 5.0 mV amplitude from 200 kHz to 0.01 Hz.

3. Results and discussion

As shown in Fig. 1(a), three samples displays the diffraction peaks at $2\theta = 14.1°$, 33.1°, 39.6°, 49.2°, 58.7°, 60.2° and 68.9°, which can be indexed to (002), (100), (103), (006), (105), (110) and (201) plane of 2H-MoS_2 (JCPDS card No. 37-1492). The 2D layered MoS_2/graphene displays broadening and lower (002) reflection, because the graphene restrains MoS_2 form well-stacking to a certain extent in *c*-direction during heat treatment [16]. According to FHWM of (002) peaks using Scherrer's equation, the layer number of MoS_2 could be estimated to be ~13, ~6 and ~10 for MoS_2, 2D MoS_2/

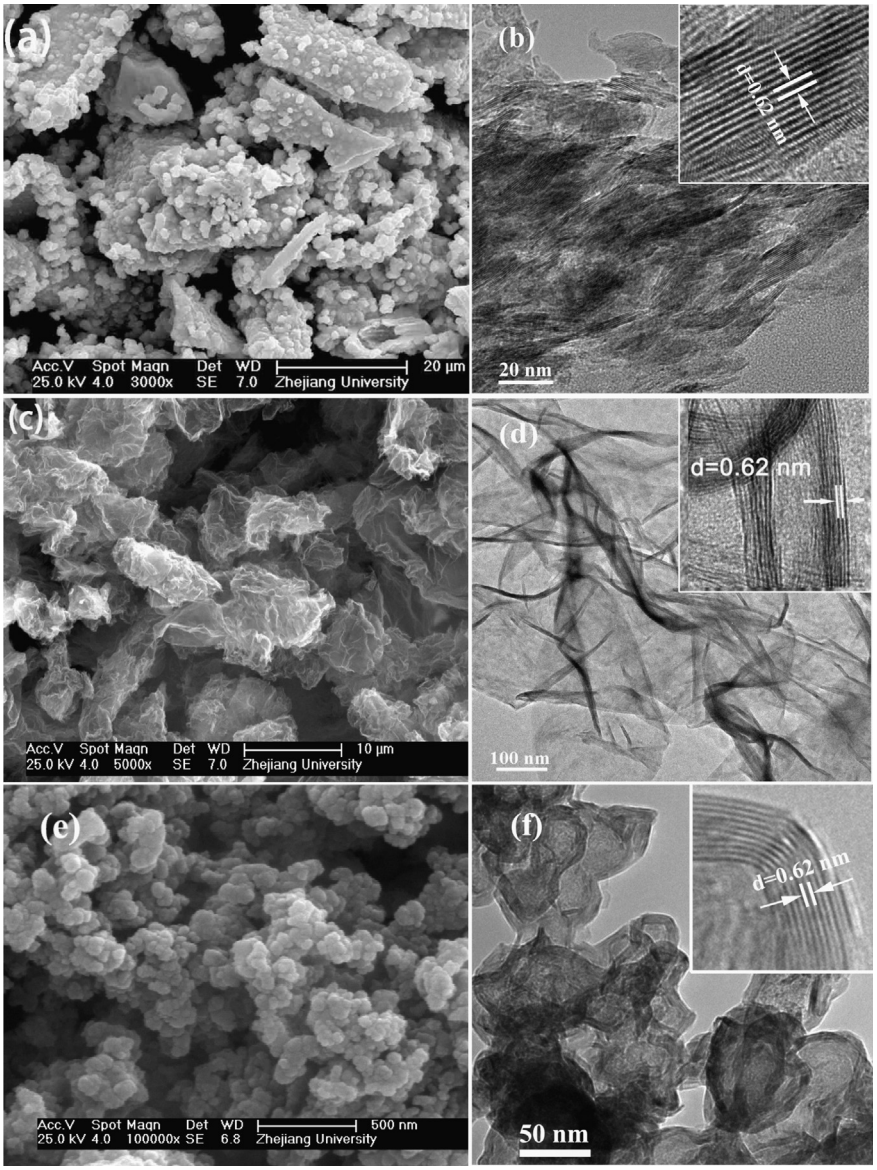

Fig. 2. SEM, TEM and HRTEM images of (a, b) the pristine MoS_2, (c, d) 2D layered MoS_2/graphene composite and (e, f) MoS_2/XC-72 composite prepared by a facile aqueous reduction after heat treatment.

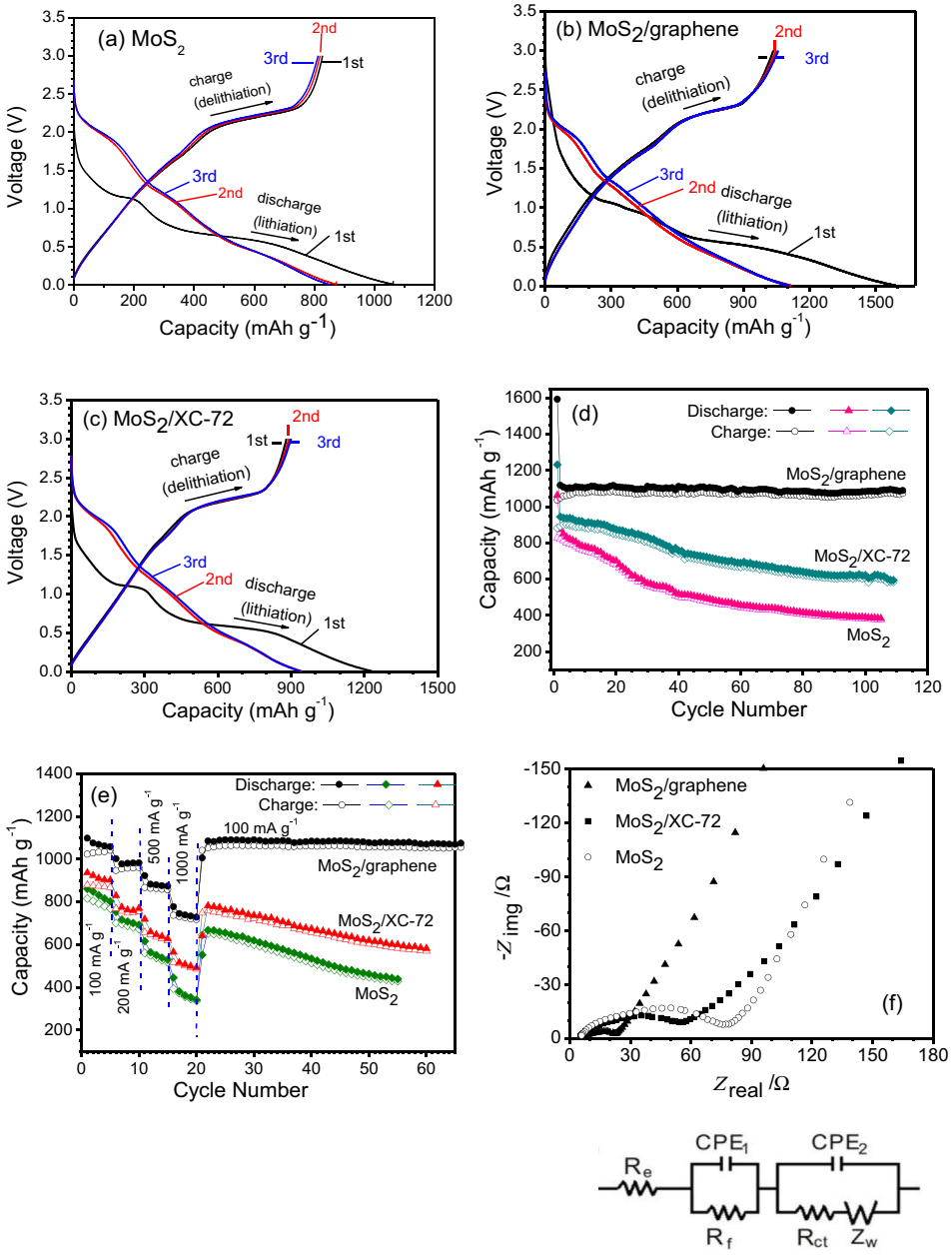

Fig. 3. (a–c) The first three charge/discharge voltage curves and (d) the cycling behaviour of the bare MoS_2, 2D layered MoS_2/graphene and MoS_2/XC-72 composite electrodes at 100 mAh g^{-1}; (e) their rate capability at different current densities; (f) the Nyquist plots of EIS obtained by applying a sine wave with amplitude of 5.0 mV over the frequency range from 200 KHz to 0.001 Hz and an equivalent circuit of the electrode, CPE is constant phase element, $Z_{CPE} = \{Q(j\omega)^n\}^{-1}$, $0 < n < 1$.

graphene and MoS_2/XC-72 composites, respectively. The elemental compositions were determined by EDX as shown in Fig. 1(b–d). The MoS_2 contains mostly Mo and S with only a trace presence of C and O. For the MoS_2/graphene and MoS_2/XC-72 composites, the presence of C is contributed from the reduced GO and XC-72 carbon. Accordingly, the presence of O is contributed from the oxygen-containing functional groups of the reduced GO and XC-72 carbon. The MoS_2 content is 79.2 wt% and 81.9 wt% for the MoS_2/graphene and MoS_2/XC-72 composites, respectively. The atomic ratio of Mo:S for all samples agrees with the stoichiometry of MoS_2.

Fig. 2(a) shows that MoS_2 displays irregular morphology consisting of nanoparticles and flakes. Its well-layered structure with $d_{(002)}$ of 0.62 nm can be clearly observed in Fig. 2(b). Fig. 2(c) shows that the 2D MoS_2/graphene composite displays a curved thin flaky appearance. Isolated MoS_2 nanoparticles or flaks are hardly found. TEM and HRTEM images of the 2D MoS_2/graphene in Fig. 2(d) clearly shows the few-layer MoS_2 sheets (5–7 layer) on the surface of the crumpled graphene. Fig. 2(e) shows that MoS_2/XC-72 displays sphere-like particles with uniform size of ~80 nm and flake-like MoS_2 is not observed. As shown in Fig. 2(f), the curved layered MoS_2 (8-10 layer) with $d_{(002)}$ of 0.62 nm well coated on the surface of XC-72 carbon nanoparticles.

Fig. 3(a–c) shows the discharge/charge voltage profiles. At the 1st discharge, the two voltage plateaus can be found at ~1.15 and ~0.60 V. The plateau at ~1.15 V is attributed to the intercalation of Li^+ into MoS_2 lattice to form Li_xMoS_2, changing the MoS_2 structure from 2H (trigonal prismatic) to 1T (octahedral) [20,21]. The plateau at ~0.60 V is due to the conversion reaction in which Li_xMoS_2 is decomposed into Mo particles and Li_2S [20–22]. In the charge process, all electrodes display a conspicuous voltage plateau at 2.2–

2.3 V, corresponding to the oxidation of Li_2S [20–22]. In the 2nd and 3rd discharge, two voltage plateaus at ~1.95 and ~1.20 V can be found, corresponding to the lithiation of S and insertion of Li^+, respectively [20–22]. At the 1st cycle, the pristine MoS_2, 2D layered MoS_2/graphene and MoS_2/XC-72 composite deliver the discharge capacity of 1063, 1592 and 1231 mAh g^{-1}, respectively. The corresponding reversible capacity is 828, 1036 and 881 mAh g^{-1} with the Coulombic efficiency of 77.9%, 65.1% and 71.6%. The irreversibility at the 1st cycle is due to irreversible processes such as the formation of SEI film, decomposition of electrolyte and reduction of oxygen-containing groups [20–22]. As shown in Fig. 3(d), the 2D layered MoS_2/graphene composite exhibits much high specific capacity with the excellent cycling stability in comparison with the pristine MoS_2 and MoS_2/XC-72. After 100 cycles, 2D MoS_2/graphene remains 1063 mAh g^{-1} with no capacity fading, while the MoS_2 and MoS_2/XC-72 electrode only remain 382 and 610 mAh g^{-1}, respectively, the corresponding capacity retention of 46.1% and 69.2%. Fig. 3(e) shows that the 2D MoS_2/graphene exhibits significantly enhanced rate capability compared to the pristine MoS_2 and MoS_2/XC-72. At a high current density of 1000 mA g^{-1}, the 2D MoS_2/graphene can deliver a reversible capacity of 732–718 mAh g^{-1}, which is much larger than that of the MoS_2 (370–335 mAh g^{-1}) and MoS_2/XC-72 (510–486 mAh g^{-1}) at the same current density. It was reported that the MoS_2/CNTs have 10% capacity fading after only 30 cycles [23] and the reversible capacity of MoS_2/CNTs were ~400 mAh g^{-1} at of 1000 mA g^{-1} [24]. Therefore, the 2D MoS_2/graphene also exhibits better cycle stability and rate capability, compared to the MoS_2/CNTs composites [23,24].

The remarkable electrochemical performance of 2D MoS_2/graphene is attributed to the outstanding properties of graphene, and synergistic interaction between 2D MoS_2 layers and graphene [12,25]. The graphene can greatly enhances the electron transfer of the electrochemical reaction and reduce the contact resistance [26]. As shown in EIS of Fig. 3(f), the high frequency semicircle could be attributed to resistance R_f and CPE_1 of the SEI film, the medium frequency semicircle to the charge-transfer resistance R_{ct} and CPE_2 of the electrode/electrolyte interface, and the inclined line in the low frequency region to Li^+ diffusion. The R_f and R_{ct} can be obtained by data fitting according to the equivalent circuit. R_f and R_{ct} of the 2D MoS_2/graphene electrode are 4.63 and 12.7 Ω, respectively, which is less than those of MoS_2 (R_f = 9.85 Ω, R_{ct} = 67.2 Ω), and these of MoS_2/XC-72 (R_f = 5.79 Ω, R_{ct} = 36.8 Ω). In particular, R_{ct} of the 2D MoS_2/graphene is much less than that of MoS_2 and MoS_2/XC-72, which demonstrates that the incorporation of graphene greatly enhances the charge transfer of the electrochemical lithiation/delithiation. In addition, the intrinsic good flexibility of graphene could effectively remain the structural stability of the composite during long-term cycle, resulting in the enhanced cycle stability.

4. Conclusions

A facile process was developed for the large-scale production of 2D layered MoS_2/graphene composites by an aqueous reduction route. It was demonstrated that MoS_2 nanosheets with ~6 layers could be dispersed very well on the surface of crumpled graphene nanosheets. The 2D MoS_2/graphene composite exhibited high Li^+ storage capacity with good cycle stability and significantly enhanced rate performance relative to pristine MoS_2 and a typical MoS_2/XC-72 composite. The satisfying electrochemical performance could be attributed to a strong suite of physical properties of graphene, and the synergistic interaction between 2D layered MoS_2 and graphene nanosheets. The tight integration between the two 2D nanosheets enabled by their geometrical similarity greatly enhanced the electron transfer processes in the composite electrode during electrochemical lithiation and delithiation.

Acknowledgements

This work was supported by the Natural Science Foundation of China (21173190), International Sci-Tech Cooperation Program of China (2012DFG42100), Doctoral Program of Higher Education of China (2011010113003), International Sci-Tech Cooperation Program of Zhejiang (2013C24011), Singapore A*STAR Project 1220203049 (R279-000-370-305), Open Fund from Zhejiang Institute of Energy and Nuclear Technology Application and Postdoctoral Fund of China (2013M540485).

References

[1] D.A.C. Brownson, D.K. Kampouris, C.E. Banks, J. Power Sources 196 (2011) 4873–4885.
[2] G.X. Wang, X.P. Shen, J. Yao, J. Park, Carbon 47 (2009) 2049–2053.
[3] E. Yoo, J. Kim, E. Hosono, H. Zhou, T. Kudo, I. Honma, Nano Lett. 8 (2008) 2277–2282.
[4] P.C. Lian, X.F. Zhu, S.Z. Liang, Z. Li, W.S. Yang, H.H. Wang, Electrochim. Acta 56 (2011) 4532–4539.
[5] S.J. Ding, D.Y. Luan, F.Y.C. Boey, J.S. Chen, X.W. Lou, Chem. Commun. 47 (2011) 7155–7157.
[6] S.M. Paek, E. Yoo, I. Honma, Nano Lett. 9 (2009) 72–75.
[7] L.W. Ji, Z. Lin, M. Alcoutlabi, X.W. Zhang, Energy Environ. Sci. 4 (2011) 2682–2699.
[8] M.H. Liang, L.J. Zhi, J. Mater. Chem. 19 (2009) 5871–5878.
[9] J. Xiao, D.W. Choi, L. Cosimbescu, P. Koech, J. Liu, J.P. Lemmon, Chem. Mater. 22 (2010) 4522–4524.
[10] G. Du, Z. Guo, S. Wang, R. Zeng, Z. Chen, H. Liu, Chem. Commun. 46 (2010) 1106–1108.
[11] H. Hwang, H. Kim, J. Cho, Nano Lett. 11 (2011) 4826–4830.
[12] K. Chang, W.X. Chen, ACS Nano 5 (2011) 4720–4728.
[13] J. Xiao, X.J. Wang, X.Q. Yang, S.D. Xun, G. Liu, P.K. Koech, J. Liu, J.P. Lemmon, Adv. Funct. Mater. 21 (2011) 2840–2846.
[14] Y. Li, H. Wang, L. Xie, Y. Liang, G. Hong, H. Dai, J. Am. Chem. Soc. 133 (2011) 7296–7299.
[15] X.S. Zhou, L.J. Wan, Y.G. Guo, Chem. Commun. 49 (2013) 1838–1840.
[16] Y.D. Ma, Y. Dai, M. Guo, C.W. Niu, B.B. Huang, Nanoscale 3 (2011) 3883–3887.
[17] A.K. Geim, I.V. Grigorieva, Nature 499 (2013) 419–425.
[18] Q.H. Wang, K. Kalantar-Zadeh, A. Kis, J.N. Coleman, M.S. Strano, Nat. Nanotechnol. 7 (2012) 699–712.
[19] W.S. Hummers, R.E. Offeman, J. Am. Chem. Soc. 80 (1958), 1339–1339.
[20] X.P. Fang, X.Q. Yu, S.F. Liao, Y.F. Shi, Y.S. Hu, Z.X. Wang, G.D. Stucky, L.Q. Chen, Microporous Mesoporous Mater. 151 (2012) 418–423.
[21] S.J. Ding, D.Y. Zhang, J.S. Chen, X.W. Lou, Nanoscale 4 (2012) 95–98.
[22] C.F. Zhang, H.B. Wu, Z.P. Guo, X.W. Lou, Electrochem. Commun. 20 (2012) 7–10.
[23] K. Bindumadhavan, S.K. Srivastava, S. Mahanty, Chem. Commun. 49 (2013) 1823–1825.
[24] Y.M. Shi, Y. Wang, J.I. Wong, A.Y.S. Tan, C.L. Hsu, L.J. Li, Y.C. Lu, H.Y. Yang, Sci. Rep. 3 (2013) 2169.
[25] X. Chen, J. He, D. Srivastava, J. Li, Appl. Phys. Lett. 100 (2012) 263901.
[26] W. Li, C. Tan, M.A. Lowe, H.D. Abruna, D.C. Ralph, ACS Nano 5 (2011) 2264–2270.